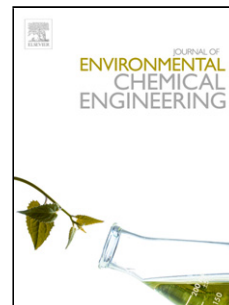


## Accepted Manuscript

Title: Adsorption of Organic Dyes from Aqueous Solutions Using Surfactant Exfoliated Graphene

Authors: Alison Y.W. Sham, Shannon M. Notley

PII: S2213-3437(17)30667-X  
DOI: <https://doi.org/10.1016/j.jece.2017.12.028>  
Reference: JECE 2075



To appear in:

Received date: 14-8-2017  
Revised date: 11-12-2017  
Accepted date: 13-12-2017

Please cite this article as: Alison Y.W. Sham, Shannon M. Notley, Adsorption of Organic Dyes from Aqueous Solutions Using Surfactant Exfoliated Graphene, Journal of Environmental Chemical Engineering <https://doi.org/10.1016/j.jece.2017.12.028>

This is a PDF file of an unedited manuscript that has been accepted for publication. As a service to our customers we are providing this early version of the manuscript. The manuscript will undergo copyediting, typesetting, and review of the resulting proof before it is published in its final form. Please note that during the production process errors may be discovered which could affect the content, and all legal disclaimers that apply to the journal pertain.

# Adsorption of Organic Dyes from Aqueous Solutions Using Surfactant Exfoliated Graphene

*Alison Y. W. Sham<sup>a</sup> and Shannon M. Notley<sup>a\*</sup>*

a) Department of Applied Mathematics, Research School of Physics and Engineering, Australian

National University, Acton 2601 ACT, Australia

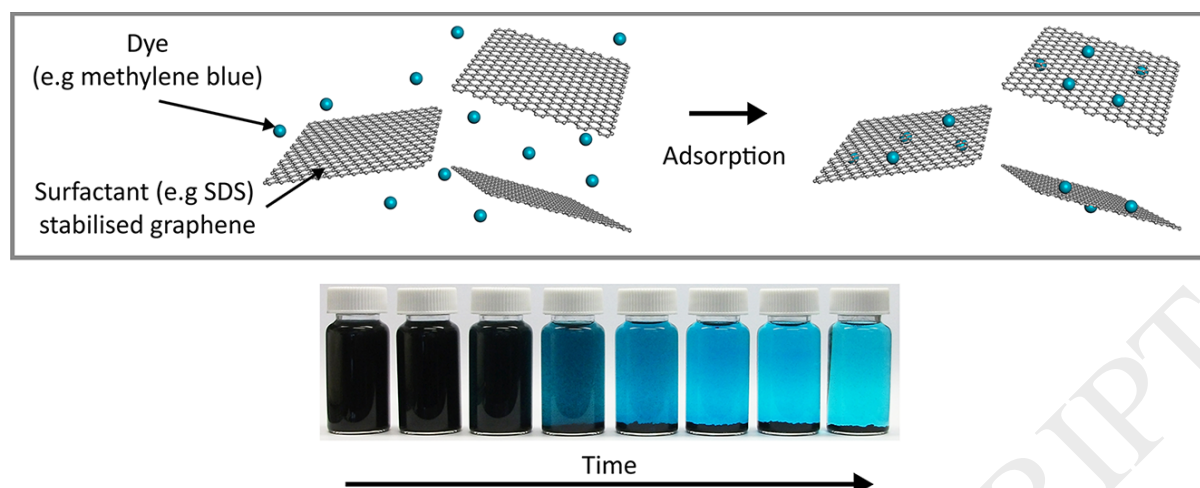
Corresponding author\*

Email: [shannon.notley@anu.edu.au](mailto:shannon.notley@anu.edu.au)

Tel: +61 2 6125 9600

Fax: +61 2 6125 0732

## Graphical Abstract



## HIGHLIGHTS

- Aqueous solutions of ionic organic dyes were adsorbed by suspensions of graphene.
- Suspensions prepared by surfactant-assisted ultrasonic exfoliation.
- Dye adsorption driven primarily by electrostatics.
- SDS exfoliated graphene maximum adsorption capacity of methylene blue: 782.3 mg/g.
- Adsorption by SDS exfoliated graphene is rapid and leads to particle aggregation.

## ABSTRACT

In this study, graphene exfoliated in the presence of surfactants was investigated as an adsorbent for the removal of organic dyes from aqueous solution. The resultant graphene particles were shown using zeta potential measurements to possess effective surface charges dominated by the charge of the adsorbed exfoliating surfactant. In this way, the overall charge on the particles, and hence the ability to adsorb dyes, was significantly enhanced compared to previously explored surfactant free systems. Furthermore, the graphene particles could be produced to have either positive or negative charge allowing the selective removal of anionic or cationic species from water respectively. The adsorption of the dyes from solution was demonstrated to be driven by electrostatic interactions with the adsorbed surfactant. The maximum removal of dye was achieved when cationic methylene blue was exposed to graphene exfoliated using the anionic surfactant, sodium dodecyl sulfate (SDS). Adsorption

of methylene blue on SDS exfoliated graphene was strongly influenced by contact time and temperature, while variations in pH were shown to have a minor effect on adsorption. Indeed, the rate of adsorption was faster than previous studies due to the inherent 2D nature of the highly exfoliated graphene particles. The adsorption data was modelled using the Freundlich and Langmuir adsorption isotherms, whilst the pseudo-second order model and the intraparticle diffusion models were used to model the kinetics of the adsorption process. SDS exfoliated graphene particles exhibited a maximum adsorption capacity of 782.3 mg/g at 25°C, greater than that of many other graphene-based materials. Thus, surfactant exfoliated graphene particles not only demonstrated excellent adsorption characteristics, but also the ability to maximize the amount of dye adsorbed based on solution conditions or the exfoliating surfactant.

**Keywords** graphene, organic dye, adsorption, Pluronic F108, surfactant

## 1. INTRODUCTION

The ability to effectively treat industrial effluent contaminated by water-soluble organic dyes is a major, ongoing environmental concern. Organic dyes are widely used as part of coloring processes in the textile [1, 2], paper [3], leather tanning [4], food [5, 6], polymer [7], cosmetics [8, 9], printing and dye manufacturing [9] industries. However, their release into the environment in processing wastewater poses a serious risk to both human health and the ecosystem, with some dyes inducing toxic [10], mutagenic [8] and carcinogenic [1] effects in humans and aquatic life. As organic dyes are generally resistant to natural degradation, it is imperative that the dyes are removed from industrial effluent using appropriate water treatment technologies prior to their discharge into the environment.

While organic dyes can be removed from the aqueous phase using a number of treatment technologies including membrane filtration and ion-exchange, one of the most effective and widespread methods available to remove dyes from wastewater is through adsorption onto carbon materials [3, 11]. Here, adsorption is driven by attractive intermolecular interactions between the contaminant molecules and the surface of the carbon material. Most conventional carbon adsorbents such as activated charcoal, are produced by either chemical or physical activation of natural, carbon-rich precursors such as coal, coconut shells, lignite, peat or wood [12], resulting in highly porous or granular structures coupled with chemically heterogeneous surfaces. The high specific surface area as well as the variety of active sites available on these adsorbents is typically credited with greater adsorption capacity and forms the basis upon which highly porous carbon adsorbents, have been studied as a means to improve dye adsorption [13]. However, the adsorption of organic dye molecules onto the surface of carbon materials has also been shown to be affected by a complex combination of interdependent factors which further influence the type and number of adsorptive interactions present, along with dye

accessibility for the active sites. These factors include the adsorbent dosage [9, 14, 15], initial dye concentration [16, 17], dye structure [14], solution pH [9, 18], ionic strength [19, 20] and temperature [9, 20, 21]. Thus, investigating the adsorption capacities of novel carbon materials offers a simple method of achieving significant improvement in the removal efficiency of water-soluble organic dyes from solution.

One type of innovative carbon material that holds great potential in the adsorption of organic dyes from solution is graphene [22]. Graphene has been the subject of significant research over the past decade due to its unique structure, which is characterized by an isolated monolayer of  $sp^2$  bonded carbon atoms arranged in a planar, hexagonal lattice [23, 24]. This 2-dimensional structure is responsible for an assortment of exceptional material properties [25-27], which could be applied to a wide variety of technologies including adsorption-based water purification. For instance, graphene is an ideal candidate for removing organic dyes from aqueous solutions due to its extremely high surface area to volume ratio and conjugated structure, which may enable effective dye adsorption at low loadings compared to conventional carbon adsorbents. Indeed, the ability for similar, graphene-based derivatives to act as effective dye adsorbents has already been recognized and investigated in several studies and reviews [28], with substantial research undertaken in the use of graphene oxide [17, 21, 29, 30], reduced graphene oxide [17, 30-32] and graphene-based nanocomposites [33-35].

Although there are a number of methods available that can be used to produce pristine graphene [36], graphene prepared through the ultrasonic exfoliation of graphite is particularly well suited to the removal of dyes from aqueous solutions. The ultrasonic exfoliation of graphite is capable of forming highly concentrated, aqueous dispersions of graphene using continuous surfactant addition which promotes exfoliation and separation of the graphite in the liquid phase [37-40]. Surfactant adsorbs onto the graphene surface, preventing reaggregation

of the graphene by imparting electrostatic and steric interactions specific to the type of surfactant employed [40]. Like other modes of producing graphene, the resulting graphene layers exhibit exceptionally high aspect ratios [41]. However, surfactant exfoliated graphene also offers a number of distinct advantages over other similar, carbon adsorbents. For instance, unlike other methods of producing pristine graphene, the ultrasonic exfoliation technique produces particles which exist in aqueous solution, enabling rapid and effective dispersion of the particles in contaminated water. By employing an appropriate ionic surfactant during the exfoliation process, the surface properties of surfactant exfoliated graphene can also be altered to promote attractive electrostatic interactions while retaining the conjugated lattice structure, which is capable of supporting Van der Waals based interactions with the aromatic portions of the dyes. Despite these features however, the adsorption capacity of surfactant exfoliated graphene with respect to contaminants such as organic dyes has yet to be explored. Therefore, it is essential that further studies into the adsorption of ionic organic dyes on surfactant exfoliated graphene are conducted in order to investigate the potential of these particles in dye removal processes.

The experiments presented in this study examine for the first time, the adsorption of organic dyes from the aqueous phase using surfactant exfoliated graphene. In this project, two organic dyes, methylene blue and methyl red were used to study the adsorption behavior of graphene particles stabilized using anionic, cationic and non-ionic surfactants. During this study, various experimental conditions were examined to determine their effect on organic dye uptake by anionic surfactant exfoliated graphene. The results of the study suggest the adsorption of organic dyes by surfactant exfoliated graphene is a rapid process driven primarily by electrostatic interactions at active sites on the adsorbent surface.

## 2. MATERIALS

Synthetic graphite powder with a nominal particle size of less than 20 $\mu$ m was used as received from Sigma Aldrich. The surfactants Pluronic® F108 (Mn ~14.6 kDa, HO(C<sub>2</sub>H<sub>4</sub>O)<sub>141</sub>(C<sub>3</sub>H<sub>6</sub>O)<sub>44</sub>(C<sub>2</sub>H<sub>4</sub>O)<sub>141</sub>H), Sodium dodecyl sulfate, (SDS, CH<sub>3</sub>(CH<sub>2</sub>)<sub>11</sub>SO<sub>4</sub>Na) and Cetyl trimethylammonium bromide (CTAB, C<sub>19</sub>H<sub>42</sub>BrN) were also obtained from Sigma Aldrich along with two organic dyes, methylene blue and methyl red sodium salt (properties given in Supplementary Material). 0.1 and 0.02  $\mu$ m syringe filters (Whatman™ Anotop™, 25mm diameter, Anopore membrane), along with 20 mL syringes obtained from VWR International. All solutions were prepared using ultra-pure water with a pH of 6.8 and resistivity of 18.2 M $\Omega$  cm. An appropriate amount of NaOH and HCl were used to adjust solutions to the required pH

### 3. METHODS

#### 3.1. Preparation of Stock Graphene Suspensions

Stock graphene suspensions were prepared via the method of ultrasonic exfoliation of graphite, with continuous surfactant addition [37]. In a typical experiment, surfactant solutions were added at a rate of approximately one drop per second to a 2% w/w suspension of graphite powder in water over 48 h. To produce graphene suspensions stabilized using SDS, a 0.1% w/w solution of SDS (999 mL) was typically added to the graphite solution. Similarly, a 10% w/w solution of Pluronic F108 (900 mL) was added at a rate of approximately one drop per second to a 2% w/w suspension (980 mL) of graphite powder in water under ultrasonication for 48 h. CTAB stabilized graphene suspensions were produced by adding a 10% w/w solution of CTAB at a rate of approximately one drop per second to a 2% w/w suspension (980 mL) of graphite powder in water under ultrasonication for 48 h. The suspensions were then centrifuged at 2500 rpm for 20 min to sediment larger, non-exfoliated graphite particles. The resulting CTAB and SDS exfoliated suspensions were dialyzed using 14 kDa dialysis tubing.



Concentrated suspensions of Pluronic F108 exfoliated graphene were prepared by evaporating the suspension at a temperature of 70 °C to approximately 5% of the original volume before being dialyzed using 100 kDa dialysis tubing. In both cases, dialysis was performed against water for a minimum of 48 h to remove unadsorbed surfactant from the stock suspension.

The concentration of graphene in the stock suspensions was obtained using the method described by Lotya et al. [40]. Samples exfoliated using SDS and CTAB were diluted by a factor of 20, while samples stabilized by Pluronic F108 were diluted by a factor of 100 before the visible light spectra measured using UV-Vis spectroscopy. Applying the Beer-Lambert Law to the absorption intensity of the samples at a wavelength of 660 nm and applying an extinction co-efficient [42],  $\epsilon$ , of 54.22 L g<sup>-1</sup> cm<sup>-1</sup>, yielded an average graphene concentration of 0.107 mg/mL, 0.954 mg/mL and 0.159 mg/mL for suspensions exfoliated using SDS, Pluronic F108 and CTAB respectively.

### 3.2. Particle Characterization

The exfoliated graphene particles were characterized using Zeta potential measurements, Raman Spectroscopy, UV-Vis Spectrophotometry and a DLS technique. The zeta potential of the graphene particles was determined using a Malvern Zetasizer Nano complete with MPT-2 autotitrator. Zeta potential measurements were performed at intervals of 0.5 pH units between pH 3.0 and 9, with pH adjustment being performed automatically using an appropriate amount of NaOH or HCl. Raman spectroscopy was conducted on the graphene particles using a Renishaw inVia Reflex spectrometer system, with 532 nm excitation laser. Samples were prepared by direct deposition of the undiluted graphene suspension onto silicon wafers and measured in the dry state. Particle sizing was performed using DLS with the Malvern Zetasizer Nano.

### 3.3. UV-Visible Spectroscopy

The main method used to analyse the concentration of organic dyes remaining in solution was UV-Vis spectroscopy. The UV-Vis spectrum of the solutions was measured using a Shimadzu 1800 UV-Vis spectrophotometer over the wavelength range of 200 - 800 nm with baseline correction.

In order to determine the concentration of organic dye solutions based on UV-Vis spectra, calibration curves of the two organic dyes were first constructed. Calibration curves were obtained for solutions of methylene blue at pH 3, 5, 7, and 9, and methyl red sodium salt at pH 5. For a typical calibration curve, a 100 mL stock solution of 1000 ppm organic dye solution was prepared then adjusted to the appropriate pH. In the case of methylene blue, 0.25 - 1.5 mL of the solution was then diluted to 100 mL with pH adjusted water to yield organic dye solutions with a concentration of 2.5, 5, 7.5, 10, 12.5, 15 ppm. For methyl red, 0.25 - 1 mL of stock solution was diluted to 100 mL to yield solutions with a dye concentration of 2.5, 5, 7 and 10 ppm. Calibration curves were constructed for each of the dyes at each pH. It was found that a linear relationship existed between the concentration and peak absorbance for each organic dye at each pH tested (See Supplementary Material).

#### 3.4. Adsorption of Dyes with Surfactant Exfoliated Graphene

SDS, Pluronic F108 and CTAB exfoliated graphene suspensions with a graphene concentration of 0.053 mg/mL were adjusted to pH 5. 22.5 mL volumes of the suspensions were then added to 0.125 mL of 1000 ppm pH 5 methylene blue or methyl red along with 2.375 mL of pH adjusted water, yielding 25 mL solutions with an initial dye concentration of 5 ppm ( $1.56 \times 10^{-5}$  M and  $1.72 \times 10^{-5}$  M respectively) and an initial graphene concentration of 0.048 mg/mL. Next, the solutions were agitated in a shaker bath at 60 rpm with a temperature of 25 °C for 48 h and filtered using a 0.02 µm pore size syringe filter. The filtrate was then analyzed using UV-Vis spectroscopy to determine the dye concentration in solution.

### 3.5. Adsorption Isotherms and Temperature Effects on Dye Adsorption

500 mL SDS exfoliated graphene suspensions were diluted to 1 L with water, and adjusted to pH 7. 22.5 mL volumes of the diluted SDS exfoliated graphene suspensions were then added to 50 mL conical flasks. Next, 0.125, 0.25, 0.5, 1.25 and 2.5 mL of pH 7 1000 ppm methylene blue, and 2.5 mL of pH 1500 ppm methylene blue were added to the suspensions, along with an appropriate amount of pH 7 adjusted water in order to give 25 mL solutions with initial dye concentrations ranging from 5 ppm to 150 ppm ( $4.70 \times 10^{-4}$  M). The flasks were stoppered and the solutions agitated at 60 rpm in a shaker bath heated to 25 °C. After 48 h, the solutions were filtered using a 0.1  $\mu$ m pore size syringe filter. The filtrate was then diluted by a factor of 2 for solutions with an initial methylene blue concentration of 20 ppm, and 10 for solutions with an initial concentration of between 50 and 150 ppm using water adjusted to pH 7. The UV-Vis spectrum for each sample was then obtained and the peak intensity of each spectrum used to determine the concentration of the organic dye from interpolation of the appropriate calibration curve. The equilibrium specific adsorption amount of methylene blue was calculated by Equation (1):

$$q_e = \frac{(C_0 - C_e)V}{W} \quad (1)$$

Where:

$q_e$	=	Equilibrium specific adsorption amount (mg/g)
$C_0$	=	Initial concentration of methylene blue in solution (mg/L)
$C_e$	=	Equilibrium concentration of methylene blue in solution (mg/L)
$V$	=	Volume of solution (L)
$W$	=	Mass of adsorbent (g)

### 3.6. Adsorption Kinetics and Effect of Contact Time on Dye Adsorption

Again, 500 mL SDS exfoliated graphene suspensions were diluted to 1 L with water and adjusted to pH 7. 90 mL volumes of the diluted suspensions were then added to 100 mL conical flasks. Next, 1, 5, and 10 mL of pH 7 1000 ppm methylene blue were added to the suspensions, along with an appropriate amount of pH 7 adjusted water in order to give 100 mL solutions with initial dye concentrations of 10, 50 and 100 ppm. The flasks were stoppered and the solutions agitated at 60 rpm in a shaker bath with a temperature of 25 °C and 35 °C over a period of 48 h. Aliquots of approximately 10 mL were then withdrawn at 10, 30, 60, 120 (2 h), 240 (4 h), 480 (6 h), 1440 (24 h) and 2880 (48 h) min and filtered using a 0.1 µm pore size syringe filter. The UV-Vis spectrum of each sample was obtained in order to determine the dye concentration. The specific adsorption amount of methylene blue for each withdrawal,  $q_t$ , was then calculated in a similar manner to Equation (1).

The effective surface charge of the graphene particles was also measured as a function of time. In a typical experiment, 45 mL of the diluted suspension along with 4.5 mL of water adjusted to pH 7 was introduced into the autotitrator flow system. Next, 0.5 mL of pH 7 1000 ppm methylene blue was added to the suspension in order to yield a 50 mL solution with initial dye concentration of 10 ppm. The zeta potential was measured over a period of 600 min, with the system monitoring the pH of the solution and applying intermittent agitation to the solution approximately every 2 min.

### 3.7. *Effect of pH on Dye Adsorption*

100 mL of SDS exfoliated graphene suspension were diluted to 200 mL with water and adjusted to pH 3, 5, 7 and 9. 22.5 mL volumes of the diluted graphene suspensions were then added to 50 mL conical flasks. Next, 1.25 mL of 1000 ppm methylene blue with corresponding pH was added to the suspensions, along with 1.25 mL of pH adjusted water, yielding 25 mL solutions with an initial dye concentration of 50 ppm. The solutions were then agitated in a shaker bath

at 60 rpm with a temperature of 25 °C for 48 h and filtered using a 0.1 µm syringe filter. A 10% v/v solution of the filtrate was then prepared and analyzed using UV-Vis spectroscopy to determine the dye concentration in solution. The equilibrium specific adsorption amount of methylene blue was then calculated.

## 4. RESULTS AND DISCUSSION

### 4.1. Characterization of Graphene

The optical, vibrational and physical properties of the exfoliated graphene particles were characterized prior to their use in subsequent adsorption experiments using UV-Vis spectroscopy, Raman spectroscopy, DLS and zeta potential measurements. The UV-Vis and Raman spectra, together with the DLS particle sizing results were used to confirm the lattice quality and size of the graphene sheets (See Supplementary Material).. The data was consistent with earlier measurements [37, 43], and was also supported by previous TEM measurements[41]. The zeta potential of graphene particles exfoliated using CTAB, Pluronic F108 and SDS were measured as a function of pH in order to determine the effective surface charge of the particles (Figure 1). These measurements are consistent with the literature pertaining to surfactant exfoliated graphene [44], where the zeta potential values of the particles are dominated by the charge imparted by the adsorbed surfactant during the exfoliation process. For instance, the graphene particles exfoliated using SDS, an anionic surfactant, exhibited a significant negative charge of between -47.5 and -66.8 mV, whilst graphene particles exfoliated using the cationic surfactant, CTAB, demonstrated a considerable positive charge of between 50.5 and 27.4 mV. In both cases, the charge exhibited by the graphene particles is consistent with the presence of strongly bound ionic surfactant molecules, despite extensive dialysis. Furthermore, these zeta potential values remain largely outside the region of colloidal instability ( $\pm 30$  mV), indicating electrostatic repulsion alone is sufficient to prevent particle

aggregation. In contrast, graphene particles exfoliated using the non-ionic surfactant, Pluronic F108, exhibited low effective surface charges of between -10.0 and -35.7 mV, which is consistent with previous studies where the particles were shown to derive colloidal stability primarily through steric effects [43]. However, regardless of the surfactant employed during the exfoliation process, the zeta potential of the graphene particles becomes progressively more negative with increasing pH. This occurs as a result of the oxygenated edge defect sites on the graphene sheets introduced during the sonication procedure [45, 46], which become deprotonated at higher pH. Collectively, these results support earlier work suggesting that highly stable suspensions of graphene particles with tailorable surface charges can be produced through the surfactant-assisted ultrasonic exfoliation of graphite using variously charged surfactants[44].

#### 4.2. *Adsorption of Ionic Dyes with Surfactant Exfoliated Graphene*

Adsorption studies were conducted using solutions of organic dye and surfactant stabilized graphene under a variety of different solution conditions. These measurements were performed to determine the effect of pH, temperature, dye concentration and contact time on the adsorption capacity of surfactant stabilized graphene particles. Experiments were also conducted in order to examine the effect of graphene particle surface charge and overall charge exhibited by the organic dye molecules on dye adsorption.

#### 4.3. *Effect of Surfactant on Dye Adsorption*

The adsorption capacity of graphene particles exfoliated using various surfactants were investigated in order to determine the primary interactions responsible for dye adsorption. In this series of experiments, 25 mL solutions initially containing either 5 ppm methyl red or methylene blue and together with 0.048 mg/mL graphene exfoliated using CTAB, Pluronic F108 and SDS at pH 5 were studied. The results of the experiments are shown in

Table 1.

Table 1 shows that each type of graphene suspension is able to remove both anionic and cationic organic dyes from solution, irrespective of surfactant used during the sonication process. The minimum amount of dye adsorbed by each type of graphene suspension is similar, varying between 22.1 and 27.9%. However, graphene suspensions prepared using a particular surfactant favor the adsorption of a particular dye. Furthermore, the type of dye favored generally exhibits an opposite charge to that of the exfoliated particles. For instance, CTAB exfoliated graphene particles adsorbed the greatest amount of methyl red, with over 50% of dye removed from solution. In contrast, SDS exfoliated graphene particles were shown to be particularly effective in the removal of the methylene blue, with less than 13.5% of dye remaining in solution following exposure to the graphene suspension. Due to this particular result, the adsorption of methylene blue by SDS exfoliated graphene was chosen as the basis for all subsequent adsorption experiments. Pluronic F108 exfoliated graphene particles were also able to remove a larger percentage of methylene blue than methyl red, albeit to a lesser extent than the SDS exfoliated graphene suspension. Thus, it is clear that the graphene suspensions exhibit different maximum adsorption capacities with respect to each of the organic dyes.

The differences in adsorption capacity are likely to be caused by the different types of intermolecular interactions possible between the surface of the graphene particles and the dye molecules. These interactions result from the three distinct areas on the graphene particles, namely the oxygen containing edge groups, the conjugated graphene structure and the adsorbed surfactant, together with the charge and structure of the dye molecules. At pH 5, the electrostatic charge of the adsorbed surfactant dominates the net effective surface charge of the graphene particles. At this pH, CTAB exfoliated graphene particles exhibit a positive charge,

the Pluronic F108 exfoliated graphene possesses a low negative charge, whilst SDS exfoliated graphene possesses a significant negative charge. Given the pKa of methylene blue and methyl red are 3.8 and 4.8 respectively [47, 48], the dye molecules exist largely in their charged states at pH 5. As a result, specific combinations of effective surface charge on the graphene particles and charge on the dyes can be used to facilitate electrostatic based interactions. In contrast, electron-rich species such as the conjugated graphene structure and aromatic systems on the organic dye molecules may enable adsorption through non-electrostatic interactions.

The ability to remove the dyes from solution, regardless of the effective surface charge on the graphene particles, is consistent with non-electrostatic interactions between the graphene surface and the dye molecules. It is likely that these interactions are comprised primarily of  $\pi$ - $\pi$  interactions, which typically exhibit greater interaction strengths than van-der Waals interactions.  $\pi$ - $\pi$  interactions have been shown previously to drive adsorption of planar aromatic compounds such as phenanthrene and biphenyl from solution onto graphene based materials [49]. As methylene blue and methyl red are both planar molecules with aromatic  $\pi$ -electron systems, they possess the required configuration to align and gain close proximity to the conjugated structure of the graphene sheets so as to facilitate  $\pi$ - $\pi$  stacking. However, the positioning of dye molecules along the graphene surface and subsequent formation of  $\pi$ - $\pi$  interactions is likely to be prevented in areas where the stabilizing surfactant is adsorbed. Consequently, the size and number of the surfactant molecules adsorbed to the carbon surface may affect the adsorption capacity of the graphene particles. This may account for the slight variation in dye adsorption observed when anionic methyl red is adsorbed using graphene exfoliated with a non-ionic and anionic surfactant.

While the adsorption measurements indicate that dye adsorption is possible through non-electrostatic interactions, the data also suggests that strong, attractive electrostatic interactions



between the dye and graphene particles promote further removal of dye from solution. Since the zeta potential measurements shown in Figure 1 indicate the electrostatic charge imparted by the ionic surfactants is distributed across the particle, it is likely areas close in proximity to the adsorbed surfactants will experience higher affinity for the dye molecules when favorable electrostatic interactions are permitted. Favorable electrostatic interactions are possible between the cationic CTAB exfoliated graphene particles and the anionic methyl red, as well as between the anionic SDS exfoliated graphene particles and the cationic methylene blue molecules. Pluronic F108 exfoliated particles are also capable of establishing attractive electrostatic interactions with cationic methylene blue, although to a lesser extent than the SDS exfoliated graphene due to the magnitude of the particle surface charge. The presence of these interactions is consistent with the results shown in

Table 1, which demonstrate that the graphene particles adsorb a greater percentage of dye when the dye exhibits an opposite charge to that of the particles. Consequently, the adsorption of organic dyes onto surfactant exfoliated graphene particles is maximized when attractive electrostatic interactions are permitted to occur.

#### 4.4. *Effect of Contact Time on Dye Adsorption*

The effect of contact time on adsorption of methylene blue onto SDS exfoliated graphene was investigated over a period of 48 h using samples with initial dye concentrations of 10, 50 and 100 ppm. The results of the adsorption measurements are shown in Figure 2.

Figure 2 indicates that adsorption of methylene blue by SDS exfoliated graphene occurs regardless of initial dye concentration and contact time. A high degree of adsorption is observed only 10 mins after contact with the dye. This was the minimum adsorption time able to be measured due to the amount of time required to filter the solutions. As the experiment

proceeds, the specific adsorbed amount of methylene blue dye generally remains constant within experimental error. This suggests that the system achieves equilibrium within the first 10 min of the experiment. The rapid rate of adsorption can be attributed to the high surface area and accessibility of adsorption sites of the graphene particles in solution that are available to participate in the adsorption process. Given the results presented earlier in Table 1, the adsorption process is likely governed by electrostatic interactions between the cationic methylene blue and anionic SDS exfoliated graphene particles. Consequently, the effective surface energy of the particles may also vary with contact time.

The zeta potential of the graphene particles was monitored during the initial stages following dye addition in order to further examine the mechanism of adsorption as a function of contact time. As shown in Figure 3, the zeta potential of the graphene particles increases from -46.3 mV during the first 240 minutes after initial contact with the dye to an approximate plateau value of -30 mV. This initial increase in zeta potential over time is again consistent with the electrostatically driven adsorption of methylene blue onto SDS exfoliated graphene particles. As the amount of cationic dye molecules adsorbed to the graphene particles increases, the number of unbalanced negative charges on the particle surface decreases, thereby increasing the overall effective surface charge. Typically, as the zeta potential enters the region of colloidal instability,  $\pm 30$  mV, repulsive electrostatic interactions are insufficient to maintain particle stability. This tendency to aggregate at low surface charges is supported by visual observations (Figure 4), which show significant aggregation after 120 min and near complete aggregation of dispersed particles after 240 min. In contrast, graphene dispersions remain stable for several months in the absence of dye.

#### 4.5. Adsorption Kinetics

The mechanism controlling the adsorption of methylene blue from solution by SDS exfoliated graphene was further investigated by modelling the adsorption kinetics of the process. The data presented in Figure 2 was analyzed using two common kinetic models, the pseudo-second order [50] and intra-particle diffusion kinetic model [51] (See Supplementary Material). The results of the kinetic models are shown in Figure 5 and Figure 6 with relevant constants and model fitting parameters given in Table 2. The pseudo-second-order model offers excellent agreement with the experimental data for all dye concentrations studied, as evidenced by the very high coefficients of determination for the linear regression. The model also predicts the equilibrium specific adsorbed amount of methylene blue accurately, with less than 2.3% difference between the experimental ( $q_{e,exp}$ ) and calculated ( $q_{e,calc}$ ) equilibrium specific adsorption amount,  $q_e$ . In contrast, the intra-particle diffusion model provides a poor description of the experimental data, with  $R^2$  values less than 0.5. In the event that the model is applicable,  $C$ , the model constant, indicates whether intraparticle diffusion is the rate controlling step in the adsorption process. Here,  $C$  is non-zero for all dye concentrations studied, indicating that adsorption of methylene blue dye onto SDS exfoliated graphene occurs through a complex adsorption mechanism instead of simple intraparticle diffusion.

#### 4.6. Effect of Temperature on Dye Adsorption

As temperature is also a critical factor in determining the adsorption capacity of a material, the effect of temperature on the adsorption of methylene blue was also investigated. The adsorption of dye onto SDS exfoliated graphene particles was studied at equilibrium using initial dye concentrations of 5, 10, 20, 50 and 100 ppm at 25, 35 and 45 °C. The results of these experiments are shown in Figure 7, where the specific adsorbed amount of methylene blue,  $q_e$ , is presented in terms of the equilibrium concentration of methylene blue in solution,  $C_e$ .

The majority of adsorption experiments described in this study were performed at 25 °C, where SDS exfoliated graphene exhibits a maximum adsorption capacity for methylene blue of 782.3 mg/g. This value is greater than that of nearly 200 other adsorbents listed in the literature[52], including various natural materials, bioadsorbents, agricultural wastes, industrial adsorbents, as well as activated carbons and coals used for commercial and research purposes. It is also greater than those of other graphene-based materials including reduced graphene oxide[53] and graphene oxide[54]. Additionally, SDS exfoliated graphene exhibited higher maximum adsorption capacities for methylene blue than several other novel adsorbent particles recently reported in the literature[55-57]. However, there remains a small number of materials which exhibit greater maximum adsorption capacities than SDS exfoliated graphene including commercial activated carbon (980.3 mg/g)[58], PMAA modified biomass of baker's yeast (869.6 mg/g)[59] and teak wood bark (914.59 mg/g)[60]. In general, these adsorbents require at least 30 minutes to achieve maximum adsorption of methylene blue, unlike the SDS exfoliated graphene particles, which have been shown to reach equilibrium within 10 minutes

(Figure 2). Thus, SDS exfoliated graphene particles exhibit excellent adsorption characteristics with respect to methylene blue at 25 °C.

From Figure 7, it is clear that an increase in temperature reduces the adsorption capacity of SDS exfoliated graphene. As the temperature increases from 25 °C to 45 °C, the maximum adsorption capacity of SDS exfoliated graphene decreases to 701.4 mg/L. Despite a reduction in adsorption capacity, these values remain far greater than other graphene-based materials such as reduced graphene oxide, which has maximum adsorption capacities ranging from 153.85 to 204.08 mg/g when the temperature is varied from 20 to 40 °C [53]. Consequently, SDS exfoliated graphene remains an effective adsorbent under different environmental temperatures. The inverse relationship between adsorption capacity and temperature such as that shown in Figure 7 is indicative of an exothermic process[61], which is consistent with the standard thermodynamics of adsorption.

#### 4.7. *Equilibrium Adsorption Isotherm*

In order to further investigate the process governing the adsorption of methylene blue onto SDS exfoliated graphene, the data presented in Figure 7 was analyzed using two frequently utilized adsorption isotherm models, the Langmuir and Freundlich adsorption isotherms (See Supplementary Material).

The Langmuir adsorption isotherm as applied to the experimental data is shown in Figure 8, with relevant constants and model fitting parameters given in Table 3. Figure 8 shows good agreement between the adsorption model and experimental data at 25 °C, which is supported by the high coefficient of determination presented in Table 3. However, the other  $R^2$  values suggest the data becomes less consistent with the Langmuir model of adsorption as the temperature increases. Additionally, the theoretical maximum specific adsorption amount,

$q_{max}$ , shown in Table 3 does not correspond well with experimental results, indicating the adsorption process is not adequately described by the Langmuir isotherm.

The Freundlich adsorption isotherm is shown in Figure 9, with relevant constants and model fitting parameters given in Table 4. Figure 9 shows reasonable agreement between the experimental data and adsorption model at all temperatures studied. This is supported by the high  $R^2$  values given in Table 4, which suggest better overall agreement with the Freundlich model than the Langmuir adsorption isotherm. Consequently, the data indicates that the surfaces of SDS exfoliated graphene particles tend to behave like heterogeneous surfaces with specific active sites during the adsorption process. Such a result is consistent with the known surface properties of surfactant exfoliated graphene, including the presence of chemically distinct species in specific areas along the surface and edges of the carbon lattice.

The relationship between temperature and the isotherm constants shown in Table 4 also suggests the experimental data is compatible with the Freundlich adsorption isotherm. As the temperature decreases, the slope of the isotherm  $\frac{1}{n}$  approaches 0, indicating the surface becomes more chemically heterogeneous [62]. This could directly reflect changes in the amount of adsorbed SDS present on the graphene surface with temperature, as the quantity of adsorbed ionic surfactant at a solid surface generally decreases at heightened temperatures due to an increase in kinetic energy of the species [63]. While  $\frac{1}{n}$  is related to surface heterogeneity, the

Freundlich exponent,  $n$ , indicates the favorability of the adsorption process, with adsorption typically occurring for  $n < 1$ . The values for  $\frac{1}{n}$  in Table 4, suggests that adsorption of the dye onto the particles is favorable at all temperatures studied, yet becomes less favorable as the temperature is increased. Given dye adsorption does occur and is likely to be driven primarily by strong electrostatic interactions involving the charged surfactant, this trend is also consistent with a reduction in the amount of surfactant adsorbed on the graphene particles as the temperature is raised. The proposed relationship between temperature and surface heterogeneity is also supported by the trend in the Freundlich adsorption constant,  $k_F$ , which is observed to decrease with increased temperature.  $k_F$  is an approximate indicator of adsorption capacity, suggesting that the adsorption capacity of surfactant exfoliated graphene particles decreases upon raising the temperature. Thus, the isotherm constants shown in Table 4 suggest the experimental data is reasonably consistent with the Freundlich adsorption isotherm model.

#### 4.8. *Effect of pH on Adsorption*

In order to determine the effect of pH on the adsorption capacity of SDS exfoliated graphene, the adsorption of methylene blue was investigated at pH 3,5,7 and 9. It was found that the specific adsorbed amount of dye varies little with pH and is well within experimental error for all pH conditions tested (See Supplementary Material).

The results of this study indicate that surfactant-exfoliated graphene holds great potential as an adsorbent for the removal of organic dyes from aqueous solutions. For instance, the minimal time required to achieve equilibrium adsorption of methylene blue coupled with the excellent adsorption capacity of SDS exfoliated graphene at 25°C are two highly attractive properties

which demonstrate the superior performance of surfactant exfoliated graphene as a carbon adsorbent. The ability for surfactant exfoliated graphene particles to aggregate upon adsorption of the dyes may also prove valuable in the separation of these nanoscale adsorbents from the liquid phase. However, a major advantage of these types of particles compared to other graphene derivatives is the ability to tailor their particle surface interactions by simply altering the type of surfactant employed in the exfoliation process. This can allow the effective, targeted removal of dyes based on electrostatic charge. For example, unlike surfactant exfoliated graphene, graphene oxide inherently possesses negative charges arising from the presence of epoxy, hydroxyl and carboxyl groups along the basal plane and has shown to be effective in adsorbing only cationic dyes[28]. Furthermore, as electrostatic interactions are the primary driver for dye adsorption onto surfactant exfoliated graphene, the particles may have the potential to remove a variety of other ionic contaminants from the aqueous phase including heavy metal ions and ionic pesticides.

## 5. CONCLUSIONS

The ability to adsorb pollutants onto carbon-based materials is a major processing technology critical to many industrial wastewater treatment operations and environmental remediation activities. It is particularly efficient at removing biologically harmful contaminants such as organic dyes which often resist degradation in aqueous mediums. In this study, surfactant exfoliated graphene particles were used to adsorb two ionic organic dyes, methylene blue and methyl red from solution. The graphene particles were prepared in the presence of a cationic, non-ionic and anionic surfactant through aqueous phase exfoliation of graphite.

At 25 °C, graphene particles stabilized by the anionic surfactant SDS demonstrated excellent adsorption of cationic methylene blue from the aqueous phase. The particles exhibited a



maximum adsorption capacity of 782.3 mg/g, greater than that of many other adsorbents in the literature. Furthermore, the adsorption of dye was found to be exceedingly rapid, reaching equilibrium within the first 10 mins of contact for all initial dye concentrations tested. Visual observations obtained throughout the adsorption process also indicated rapid particle aggregation, which was attributed to a reduction in electrostatic particle stabilization using corresponding zeta potential measurements. This feature could enable rapid separation of the particles from solution through either sedimentation or filtration.

The main mechanism responsible for the adsorption of methylene blue onto SDS exfoliated graphene was analyzed using a series of theoretical models, while the effect of solution conditions on adsorption were also investigated. In particular, the temperature of the solution had a significant influence on dye removal, with lower temperatures favoring dye adsorption. Conversely, adsorption capacity showed little variation with pH, indicating the attractive interactions between the oxygenated edge groups and dye had a negligible effect on the amount of methylene blue adsorbed. Meanwhile, the experimental kinetic data provided excellent agreement with the adsorption parameters predicted using the pseudo-second order kinetics model. The results from the adsorption experiments were also consistent with the Freundlich adsorption isotherm, suggesting adsorption of methylene blue at active sites along the chemically heterogeneous SDS exfoliated graphene surface.

The adsorption of methylene blue and methyl red by surfactant exfoliated graphene was shown to be highly dependent on the charge of the stabilizing surfactant. Zeta potential measurements indicated that the overall effective surface charge of these particles was dominated by the electrostatic charge on the stabilizing surfactant. In the case of the non-ionic surfactant, particle surface charge was largely influenced by the presence of negatively charged oxygenated edge groups. The percentage of dye removed by each type of surfactant stabilized

graphene was maximized when the dye and graphene surface was exhibited opposite charges. This adsorption behavior was primarily attributed to attractive electrostatic interactions between the ionic dyes and surfactants, with weaker,  $\pi$ - $\pi$  interactions playing a secondary role in dye adsorption. altering dye-particle interactions through changes in processing conditions enabled overall changes in adsorption efficiency. Thus, the results of these experiments collectively illustrate the potential of surfactant exfoliated graphene to act as an effective carbon-based adsorbent.

#### Acknowledgements

Funding: This research is supported by an Australian Government Research Training Program (RTP) Scholarship.

## REFERENCES

- [1] R.O. Alves de Lima, A.P. Bazo, D.M.F. Salvadori, C.M. Rech, D. de Palma Oliveira, G. de Aragão Umbuzeiro, Mutagenic and carcinogenic potential of a textile azo dye processing plant effluent that impacts a drinking water source, *Mutation Research/Genetic Toxicology and Environmental Mutagenesis* 626 (2007) 53-60.
- [2] Y. Al-Degs, M.A.M. Khraisheh, S.J. Allen, M.N. Ahmad, Effect of carbon surface chemistry on the removal of reactive dyes from textile effluent, *Water Res.* 34 (2000) 927-935.
- [3] V.K. Gupta, Suhas, Application of low-cost adsorbents for dye removal – A review, *Journal of Environmental Management* 90 (2009) 2313-2342.
- [4] J.S. Piccin, C.S. Gomes, B. Mella, M. Gutterres, Color removal from real leather dyeing effluent using tannery waste as an adsorbent, *Journal of Environmental Chemical Engineering* 4 (2016) 1061-1067.
- [5] M. Shabandokht, E. Binaeian, H.-A. Tayebi, Adsorption of food dye Acid red 18 onto polyaniline-modified rice husk composite: isotherm and kinetic analysis, *Desalination and Water Treatment* 57 (2016) 27638-27650.
- [6] M.A. Al-Ghouti, A.A. Issa, B.S. Al-Saqarat, A.Y. Al-Reyahi, Y.S. Al-Degs, Multivariate analysis of competitive adsorption of food dyes by activated pine wood, *Desalination and Water Treatment* 57 (2016) 27651-27662.
- [7] C. Fleischmann, M. Lievenbrück, *Polymers and Dyes: Developments and Applications*, *Polymers* 7 (2015) 717-746.
- [8] K.-T. Chung, C.E. Cerniglia, Mutagenicity of Azo Dyes: Structure-Activity Relationships, *Mutation Research/Reviews in Genetic Toxicology* 277 (1992) 201-220.
- [9] M.T. Yagub, T.K. Sen, S. Afroze, H.M. Ang, Dye and its removal from aqueous solution by adsorption: A review, *Adv. Colloid Interface Sci.* 209 (2014) 172-184.

- [10] T. Robinson, G. McMullan, R. Marchant, P. Nigam, Remediation of dyes in textile effluent: a critical review on current treatment technologies with a proposed alternative, *Bioresour. Technol.* 77 (2001) 247-255.
- [11] G. Crini, Non-conventional low-cost adsorbents for dye removal: A review, *Bioresour. Technol.* 97 (2006) 1061-1085.
- [12] D. Mohan, C.U. Pittman Jr, Arsenic removal from water/wastewater using adsorbents—A critical review, *J. Hazard. Mater.* 142 (2007) 1-53.
- [13] S.K. Ling, H.Y. Tian, S. Wang, T. Rufford, Z.H. Zhu, C.E. Buckley, KOH catalysed preparation of activated carbon aerogels for dye adsorption, *J. Colloid Interface Sci.* 357 (2011) 157-162.
- [14] H. Altaher, T.E. Khalil, R. Abubeah, The effect of dye chemical structure on adsorption on activated carbon: a comparative study, *Color. Technol.* 130 (2014) 205-214.
- [15] W. Yang, D. Wu, R. Fu, Effect of surface chemistry on the adsorption of basic dyes on carbon aerogels, *Colloids and Surfaces A: Physicochemical and Engineering Aspects* 312 (2008) 118-124.
- [16] K.A. Adegoke, O.S. Bello, Dye sequestration using agricultural wastes as adsorbents, *Water Resources and Industry* 12 (2015) 8-24.
- [17] G.K. Ramesha, A. Vijaya Kumara, H.B. Muralidhara, S. Sampath, Graphene and graphene oxide as effective adsorbents toward anionic and cationic dyes, *J. Colloid Interface Sci.* 361 (2011) 270-277.
- [18] Y.S. Al-Degs, M.I. El-Barghouthi, A.H. El-Sheikh, G.M. Walker, Effect of solution pH, ionic strength, and temperature on adsorption behavior of reactive dyes on activated carbon, *Dyes Pigm.* 77 (2008) 16-23.

- [19] D.A. Giannakoudakis, G.Z. Kyzas, A. Avranas, N.K. Lazaridis, Multi-parametric adsorption effects of the reactive dye removal with commercial activated carbons, *J. Mol. Liq.* 213 (2016) 381-389.
- [20] J. Ghasemi, S. Asadpour, Thermodynamics' study of the adsorption process of methylene blue on activated carbon at different ionic strengths, *The Journal of Chemical Thermodynamics* 39 (2007) 967-971.
- [21] W. Zhang, C. Zhou, W. Zhou, A. Lei, Q. Zhang, Q. Wan, B. Zou, Fast and Considerable Adsorption of Methylene Blue Dye onto Graphene Oxide, *Bull. Environ. Contam. Toxicol.* 87 (2011) 86.
- [22] J. Texter, Graphene oxide and graphene flakes as stabilizers and dispersing aids, *Curr. Opin. Colloid Interface Sci.* 20 (2015) 454-464.
- [23] A.K. Geim, K.S. Novoselov, The rise of graphene, *Nat. Mater.* 6 (2007) 183-191.
- [24] K.S. Novoselov, A.K. Geim, S.V. Morozov, D. Jiang, Y. Zhang, S.V. Dubonos, I.V. Grigorieva, A.A. Firsov, Electric Field Effect in Atomically Thin Carbon Films, *Science* 306 (2004) 666-669.
- [25] K.I. Bolotin, K.J. Sikes, Z. Jiang, M. Klima, G. Fudenberg, J. Hone, P. Kim, H.L. Stormer, Ultrahigh electron mobility in suspended graphene, *Solid State Commun.* 146 (2008) 351-355.
- [26] C. Lee, X. Wei, J.W. Kysar, J. Hone, Measurement of the Elastic Properties and Intrinsic Strength of Monolayer Graphene, *Science* 321 (2008) 385-388.
- [27] K.M.F. Shahil, A.A. Balandin, Thermal properties of graphene and multilayer graphene: Applications in thermal interface materials, *Solid State Commun.* 152 (2012) 1331-1340.
- [28] M. Yusuf, F.M. Elfghi, S.A. Zaidi, E.C. Abdullah, M.A. Khan, Applications of graphene and its derivatives as an adsorbent for heavy metal and dye removal: a systematic and comprehensive overview, *RSC Advances* 5 (2015) 50392-50420.

- [29] W. Konicki, M. Aleksandrak, E. Mijowska, Equilibrium, kinetic and thermodynamic studies on adsorption of cationic dyes from aqueous solutions using graphene oxide, *Chem. Eng. Res. Des.* 123 (2017) 35-49.
- [30] D. Robati, M. Rajabi, O. Moradi, F. Najafi, I. Tyagi, S. Agarwal, V.K. Gupta, Kinetics and thermodynamics of malachite green dye adsorption from aqueous solutions on graphene oxide and reduced graphene oxide, *J. Mol. Liq.* 214 (2016) 259-263.
- [31] C. Minitha, M. Lalitha, Y. Jeyachandran, L. Senthilkumar, R.R. Kumar, Adsorption behaviour of reduced graphene oxide towards cationic and anionic dyes: Co-action of electrostatic and  $\pi - \pi$  interactions, *Mater. Chem. Phys.* 194 (2017) 243-252.
- [32] P. Sharma, B.K. Saikia, M.R. Das, Removal of methyl green dye molecule from aqueous system using reduced graphene oxide as an efficient adsorbent: Kinetics, isotherm and thermodynamic parameters, *Colloids and Surfaces A: Physicochemical and Engineering Aspects* 457 (2014) 125-133.
- [33] R. Krishna, D.M. Fernandes, C. Dias, C. Freire, J. Ventura, E. Titus, Facile synthesis of Co/RGO nanocomposite for methylene blue dye removal, *Materials Today: Proceedings* 3 (2016) 2814-2821.
- [34] S. Jayanthi, N. KrishnaRao Eswar, S.A. Singh, K. Chatterjee, G. Madras, A.K. Sood, Macroporous three-dimensional graphene oxide foams for dye adsorption and antibacterial applications, *RSC Advances* 6 (2016) 1231-1242.
- [35] Z. Geng, Y. Lin, X. Yu, Q. Shen, L. Ma, Z. Li, N. Pan, X. Wang, Highly efficient dye adsorption and removal: a functional hybrid of reduced graphene oxide-Fe<sub>3</sub>O<sub>4</sub> nanoparticles as an easily regenerative adsorbent, *J. Mater. Chem.* 22 (2012) 3527-3535.
- [36] A.C. Ferrari, F. Bonaccorso, V. Fal'ko, K.S. Novoselov, S. Roche, P. Boggild, S. Borini, F.H.L. Koppens, V. Palermo, N. Pugno, J.A. Garrido, R. Sordan, A. Bianco, L. Ballerini, M.

Prato, E. Lidorikis, J. Kivioja, C. Marinelli, T. Ryhanen, A. Morpurgo, J.N. Coleman, V. Nicolosi, L. Colombo, A. Fert, M. Garcia-Hernandez, A. Bachtold, G.F. Schneider, F. Guinea, C. Dekker, M. Barbone, Z. Sun, C. Galiotis, A.N. Grigorenko, G. Konstantatos, A. Kis, M. Katsnelson, L. Vandersypen, A. Loiseau, V. Morandi, D. Neumaier, E. Treossi, V. Pellegrini, M. Polini, A. Tredicucci, G.M. Williams, B. Hee Hong, J.-H. Ahn, J. Min Kim, H. Zirath, B.J. van Wees, H. van der Zant, L. Occhipinti, A. Di Matteo, I.A. Kinloch, T. Seyller, E. Quesnel, X. Feng, K. Teo, N. Rupesinghe, P. Hakonen, S.R.T. Neil, Q. Tannock, T. Lofwander, J. Kinaret, Science and technology roadmap for graphene, related two-dimensional crystals, and hybrid systems, *Nanoscale* 7 (2015) 4598-4810.

[37] S.M. Notley, Highly concentrated aqueous suspensions of graphene through ultrasonic exfoliation with continuous surfactant addition, *Langmuir* 28 (2012) 14110-14113.

[38] J.N. Coleman, M. Lotya, A. O'Neill, S.D. Bergin, P.J. King, U. Khan, K. Young, A. Gaucher, S. De, R.J. Smith, I.V. Shvets, S.K. Arora, G. Stanton, H.-Y. Kim, K. Lee, G.T. Kim, G.S. Duesberg, T. Hallam, J.J. Boland, J.J. Wang, J.F. Donegan, J.C. Grunlan, G. Moriarty, A. Shmeliov, R.J. Nicholls, J.M. Perkins, E.M. Grieveson, K. Theuwissen, D.W. McComb, P.D. Nellist, V. Nicolosi, Two-Dimensional Nanosheets Produced by Liquid Exfoliation of Layered Materials, *Science* 331 (2011) 568-571.

[39] J.N. Coleman, Liquid Exfoliation of Defect-Free Graphene, *Acc. Chem. Res.* 46 (2013) 14-22.

[40] M. Lotya, Y. Hernandez, P.J. King, R.J. Smith, V. Nicolosi, L.S. Karlsson, F.M. Blighe, S. De, Z. Wang, I.T. McGovern, G.S. Duesberg, J.N. Coleman, Liquid Phase Production of Graphene by Exfoliation of Graphite in Surfactant/Water Solutions, *J. Am. Chem. Soc.* 131 (2009) 3611-3620.

- [41] A.Y.W. Sham, S.M. Notley, Foam stabilisation using surfactant exfoliated graphene, *J. Colloid Interface Sci.* 469 (2016) 196-204.
- [42] V. Chabot, B. Kim, B. Sloper, C. Tzoganakis, A. Yu, High yield production and purification of few layer graphene by Gum Arabic assisted physical sonication, *Sci. Rep.* 3 (2013) 1-7.
- [43] A.Y.W. Sham, S.M. Notley, Layer-by-Layer Assembly of Thin Films Containing Exfoliated Pristine Graphene Nanosheets and Polyethyleneimine, *Langmuir* 30 (2014) 2410-2418.
- [44] R.J. Smith, M. Lotya, J.N. Coleman, The importance of repulsive potential barriers for the dispersion of graphene using surfactants, *New J. Phys.* 12 (2010) 1367-2630.
- [45] A. Griffith, S.M. Notley, pH dependent stability of aqueous suspensions of graphene with adsorbed weakly ionisable cationic polyelectrolyte, *J. Colloid Interface Sci.* 369 (2012) 201-215.
- [46] S.M. Notley, Adsorption of polyelectrolyte modified single layer graphene to silica surfaces: monolayers and multilayers, *J. Colloid Interface Sci.* 375 (2012) 35-40.
- [47] R. Qiu, S. Yin, X. Zhang, J. Xia, X. Xu, S. Luo, Synthesis and structure of an air-stable cationic organobismuth complex and its use as a highly efficient catalyst for the direct diastereoselective Mannich reaction in water, *Chem. Commun. (Cambridge, U. K.)* (2009) 4759-4761.
- [48] A.A. Spagnoli, D.A. Giannakoudakis, S. Bashkova, Adsorption of methylene blue on cashew nut shell based carbons activated with zinc chloride: The role of surface and structural parameters, *J. Mol. Liq.* 229 (2017) 465-471.



- [49] O.G. Apul, Q. Wang, Y. Zhou, T. Karanfil, Adsorption of aromatic organic contaminants by graphene nanosheets: Comparison with carbon nanotubes and activated carbon, *Water Res.* 47 (2013) 1648-1654.
- [50] Y.S. Ho, G. McKay, Pseudo-second order model for sorption processes, *Process Biochem.* (Amsterdam, Neth.) 34 (1999) 451-465.
- [51] H. Qiu, L. Lv, B.C. Pan, Q.J. Zhang, W.M. Zhang, Q.X. Zhang, Critical review in adsorption kinetic models, *Journal of Zhejiang University SCIENCE A* 10 (2009) 716-724.
- [52] M. Rafatullah, O. Sulaiman, R. Hashim, A. Ahmad, Adsorption of methylene blue on low-cost adsorbents: A review, *J. Hazard. Mater.* 177 (2010) 70-80.
- [53] T. Liu, Y. Li, Q. Du, J. Sun, Y. Jiao, G. Yang, Z. Wang, Y. Xia, W. Zhang, K. Wang, H. Zhu, D. Wu, Adsorption of methylene blue from aqueous solution by graphene, *Colloids and Surfaces B: Biointerfaces* 90 (2012) 197-203.
- [54] S.-T. Yang, S. Chen, Y. Chang, A. Cao, Y. Liu, H. Wang, Removal of methylene blue from aqueous solution by graphene oxide, *J. Colloid Interface Sci.* 359 (2011) 24-29.
- [55] F. Wang, L. Zhang, Y. Wang, X. Liu, S. Rohani, J. Lu, Fe<sub>3</sub>O<sub>4</sub>@SiO<sub>2</sub>@CS-TETA functionalized graphene oxide for the adsorption of methylene blue (MB) and Cu(II), *Appl. Surf. Sci.* 420 (2017) 970-981.
- [56] X. Liu, A. Jin, Y. Jia, T. Xia, C. Deng, M. Zhu, C. Chen, X. Chen, Synergy of adsorption and visible-light photocatalytic degradation of methylene blue by a bifunctional Z-scheme heterojunction of WO<sub>3</sub>/g-C<sub>3</sub>N<sub>4</sub>, *Appl. Surf. Sci.* 405 (2017) 359-371.
- [57] Z. Du, Y. Zhang, Z. Li, H. Chen, Y. Wang, G. Wang, P. Zou, H. Chen, Y. Zhang, Facile one-pot fabrication of nano-Fe<sub>3</sub>O<sub>4</sub>/carboxyl-functionalized baker's yeast composites and their application in methylene blue dye adsorption, *Appl. Surf. Sci.* 392 (2017) 312-320.

- [58] N. Kannan, M.M. Sundaram, Kinetics and mechanism of removal of methylene blue by adsorption on various carbons—a comparative study, *Dyes Pigm.* 51 (2001) 25-40.
- [59] J.-X. Yu, B.-H. Li, X.-M. Sun, J. Yuan, R.-a. Chi, Polymer modified biomass of baker's yeast for enhancement adsorption of methylene blue, rhodamine B and basic magenta, *J. Hazard. Mater.* 168 (2009) 1147-1154.
- [60] G. McKay, J.F. Porter, G.R. Prasad, The Removal of Dye Colours from Aqueous Solutions by Adsorption on Low-cost Materials, *Water, Air, Soil Pollut.* 114 (1999) 423-438.
- [61] B.K. Nandi, A. Goswami, M.K. Purkait, Removal of cationic dyes from aqueous solutions by kaolin: Kinetic and equilibrium studies, *Appl. Clay Sci.* 42 (2009) 583-590.
- [62] K.Y. Foo, B.H. Hameed, Insights into the modeling of adsorption isotherm systems, *Chem. Eng. J. (Lausanne)* 156 (2010) 2-10.
- [63] S. Paria, K.C. Khilar, A review on experimental studies of surfactant adsorption at the hydrophilic solid–water interface, *Adv. Colloid Interface Sci.* 110 (2004) 75-95.

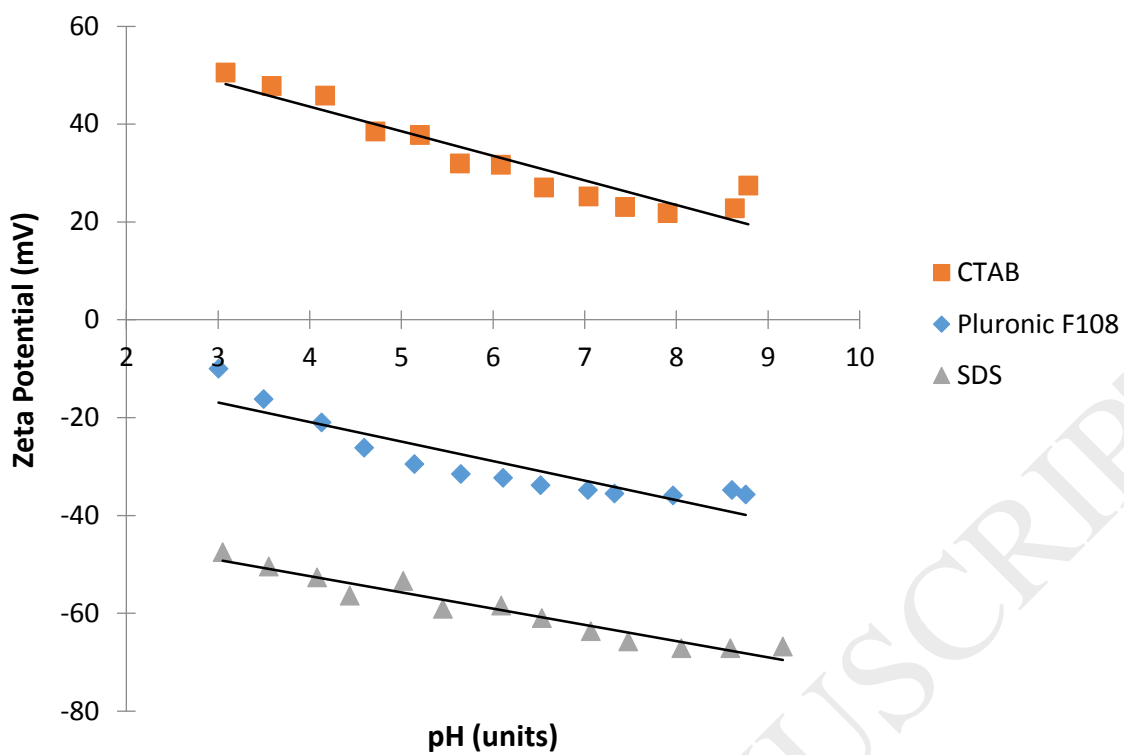


**Figure 1:** Zeta potential measurement of graphene exfoliated using CTAB, Pluronic F108 and SDS in  $\text{NaCl } 10^{-4}$  M.

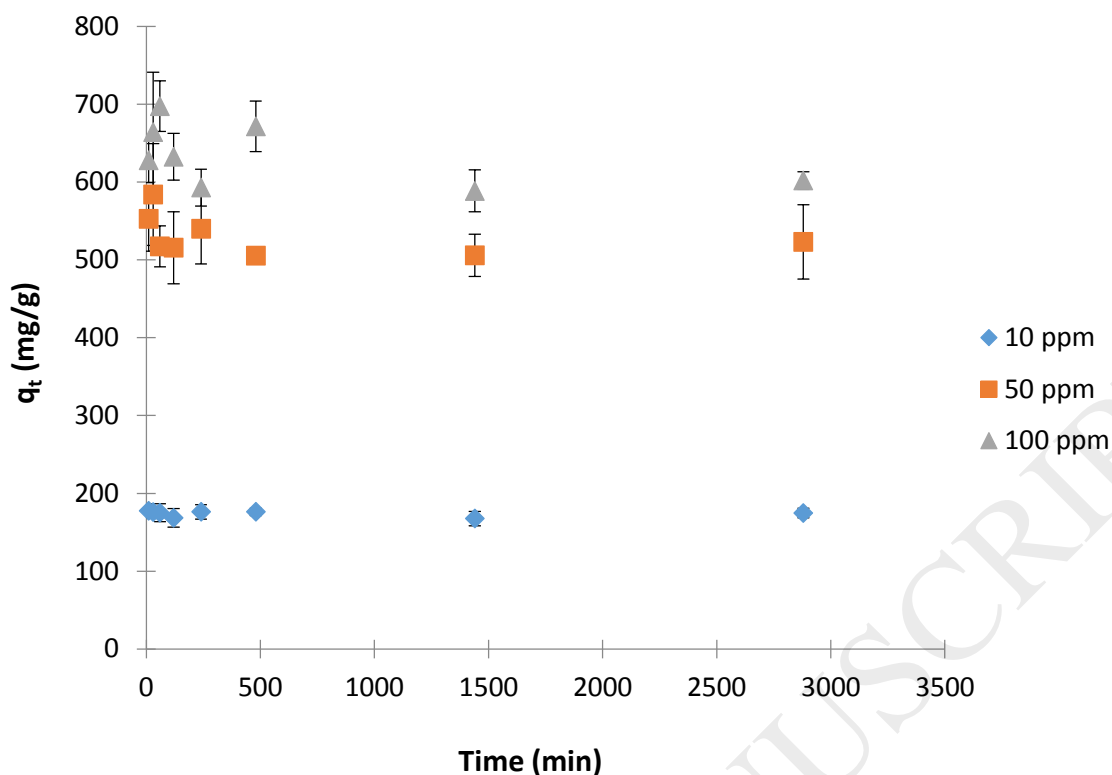


**Figure 2:** The effect of contact time on the specific adsorption amount of methylene blue on SDS exfoliated graphene particles at various dye concentrations at 25 °C.

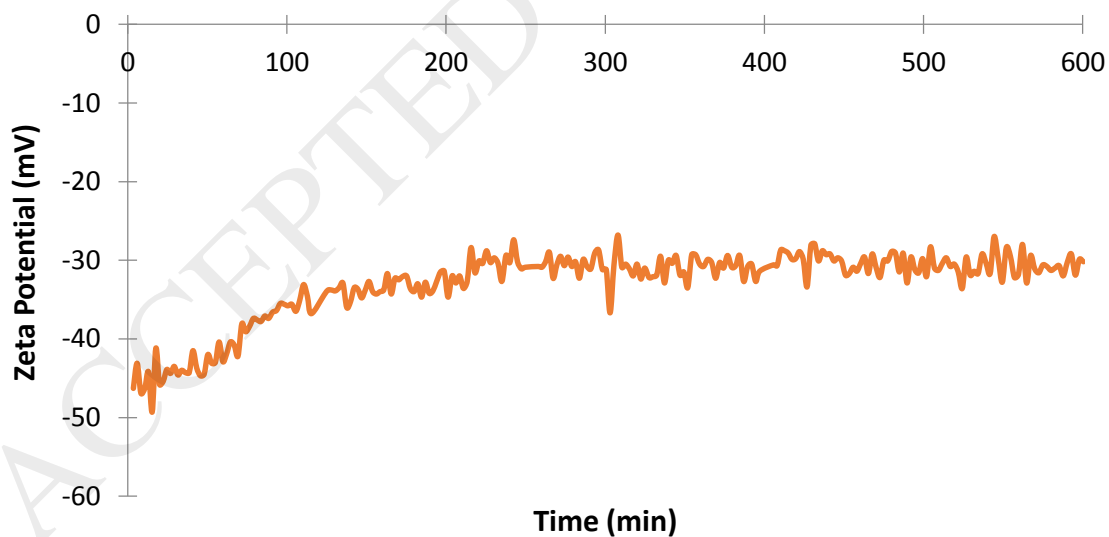


**Figure 3:** Zeta potential measurement of SDS exfoliated graphene suspension with 10 ppm methylene blue as a function of time at 25 °C.



**Figure 4:** Suspensions of SDS exfoliated graphene with 10 ppm methylene blue 10, 30, 60 min, 120, 240, 480, 1140 and 2880 min after initial contact with dye at 25 °C.

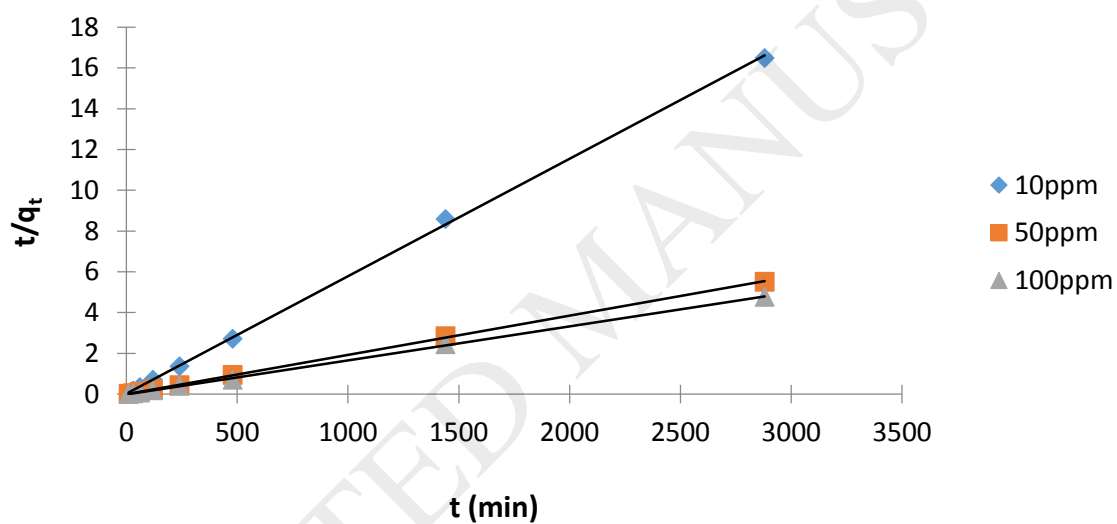


**Figure 5:** Pseudo-second order model adsorption kinetics for methylene blue adsorbed onto SDS exfoliated graphene, where  $t$  is contact time and  $q_t$  is the specific adsorption amount at  $t$ .

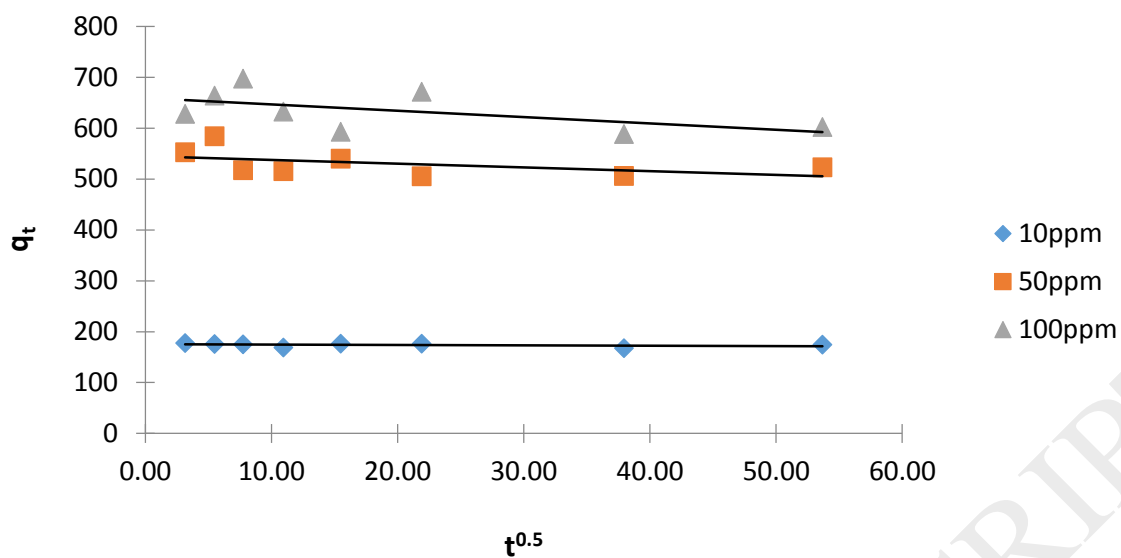


**Figure 6:** Intra-particle diffusion model adsorption kinetics for methylene blue adsorbed onto SDS exfoliated graphene.

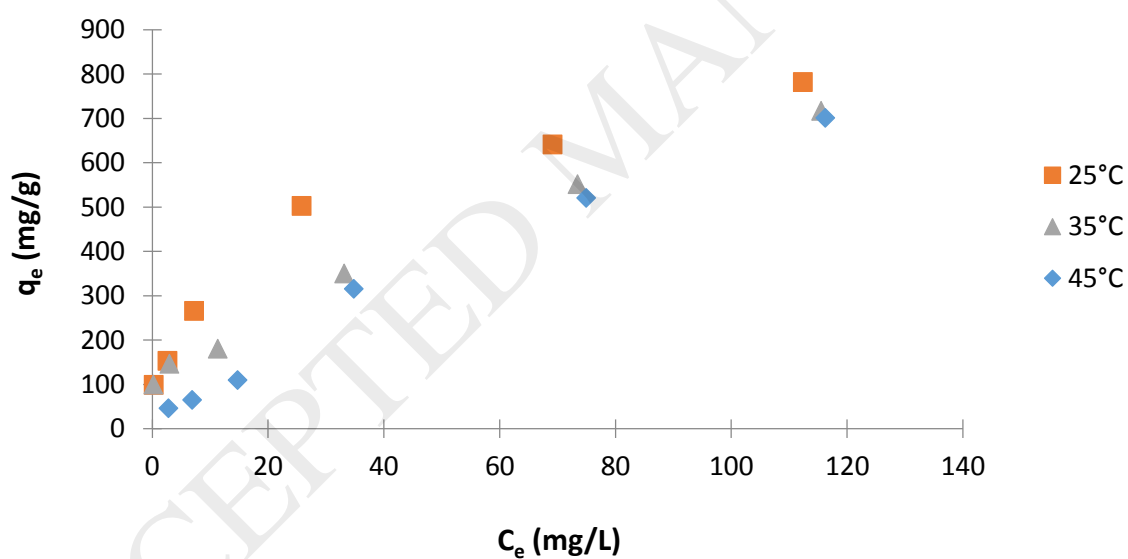


**Figure 7:** The effect of temperature on the adsorption of pH 7 methylene blue on SDS exfoliated graphene particles.

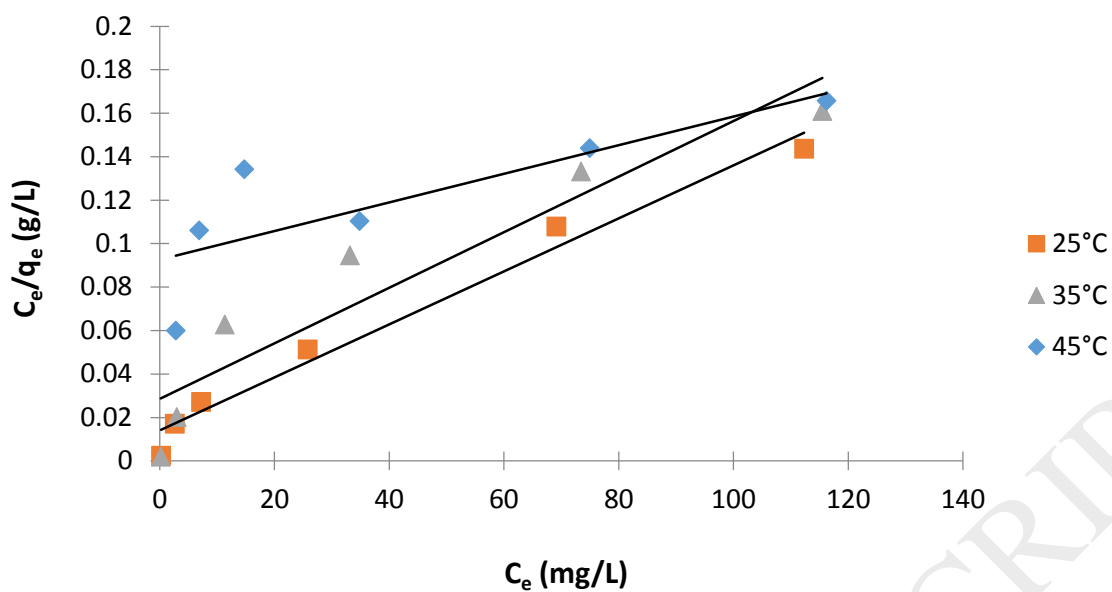


**Figure 8:** Langmuir adsorption isotherms for methylene blue on SDS exfoliated graphene particles.

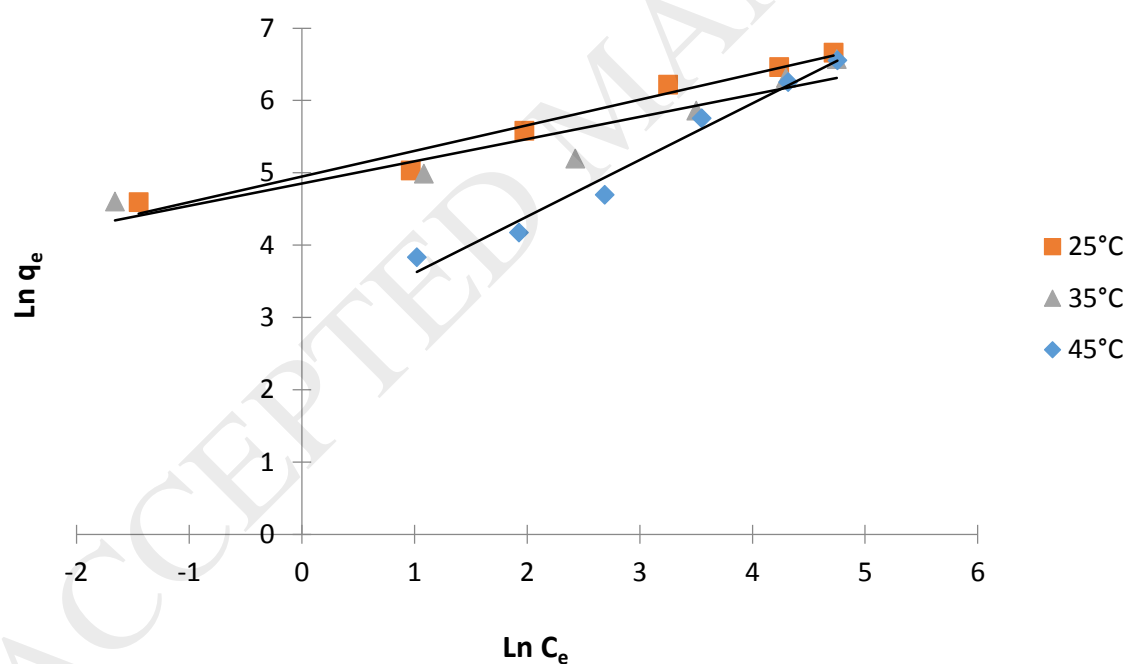


**Figure 9:** Freundlich adsorption isotherms for methylene blue on SDS exfoliated graphene particles.

**Table 1:** Percentage of organic dye removed from solution by graphene particles produced using surfactants with different electronic characteristics at pH 5.

Surfactant	Methyl Red Removal	Methylene Blue
	Efficiency (%)	Removal Efficiency (%)
CTAB	55.0	22.1
Pluronic F108	23.5	38.9
SDS	27.9	86.5

**Table 2:** Kinetic parameters for pseudo-second order model and intra-particle diffusion model, where  $C_0$  is the initial dye concentration,  $k_2$  is the pseudo-second order rate constant,  $k_p$  is the intraparticle diffusion rate constant.

$C_0$ (ppm)	Pseudo-second order				Intra-Particle Diffusion		
	$q_{e,exp}$	$q_{e,calc}$	$k_2$	$R^2$	$k_p$	$C$	$R^2$
	(mg/g)	(mg/g)	(min <sup>-1</sup> )		(mg g <sup>-1</sup> min <sup>-0.5</sup> )	(mg/g)	
10	147.72	172.41	0.000967	0.9996	-0.0689	175.36	0.1051
50	523.00	526.31	0.000269	0.9997	-0.7409	544.93	0.2364
100	602.00	588.23	-0.00011	0.9995	-1.238	658.82	0.3026

**Table 3:** Langmuir adsorption isotherm constants and model fitting parameters, where  $k_L$  is the Langmuir constant.

Temperature (°C)	$q_{max}$ (mg/g)	$k_L$ (L/g)	$R^2$
------------------	------------------	-------------	-------



25	833.33	0.085	0.9781
35	769.23	0.046	0.8896
45	1428.57	0.008	0.6550

**Table 4:** Freundlich adsorption isotherm constants and model fitting parameters.

Temperature (°C)	$1/n$	$k_F$	
		(mg/g)	$R^2$
25	0.354	4.95	0.9667
35	0.307	4.85	0.8809
45	0.782	2.83	0.9767